Molecular Genetics and Metabolism Reports 26 (2021) 100712

Contents lists available at ScienceDirect

Molecular Genetics and Metabolism Reports

journal homepage: www.elsevier.com/locate/ymgmr

Case Report

Transcriptome from opaque cornea of Fanconi anemia patient uncovers fibrosis and two connected players

Bharesh K. Chauhan [a,b,*], Anagha Medsinge [a], Hannah L. Scanga [a], Charleen T. Chu [c], Ken K. Nischal [a,b]

[a] UPMC Eye Center, Children's Hospital of Pittsburgh, Pittsburgh, PA 15224, USA
[b] Department of Ophthalmology, University of Pittsburgh School of Medicine, Pittsburgh, PA 15213, USA
[c] Department of Pathology, University of Pittsburgh School of Medicine, Pittsburgh, PA 15213, USA

ARTICLE INFO

Keywords:
Corneal opacity
Transcriptome analysis
Fibrosis
Basement membrane disruption
Glycosaminoglycans

ABSTRACT

Congenital corneal opacities (CCO) are a group of blinding corneal disorders, where the underlying molecular mechanisms are poorly understood. Phenotyping through specialized imaging and histopathology analysis, together with assessment of key transcriptomic changes (including glycosaminoglycan metabolic enzymes) in cornea(s) with CCO from a case of Fanconi anemia is the approach taken in this study to identify causal mechanisms. Based on our findings, we propose a novel mechanism and two key players contributing to CCO.

1. Introduction

Congenital corneal opacities (CCO) are rare corneal conditions with an incidence of about 2.2–3 per 100,000 [1,2]. It can be divided into primary and secondary corneal diseases [3], where the former are congenital and latter can either be congenital or acquired. Corneal transplantation is the standard treatment modality. However, they have a particularly high failure rate in the pediatric population due to complications such as rejection, infection, scar formation, or glaucoma [4]. Alternative treatment modalities are therefore clearly needed through better understanding of CCO at the molecular level.

Diagnosis of CCO sub-types has significantly improved through imaging techniques [2,3,5–7]. An early report found 40% of CCO diagnoses were incorrect when evaluated by ultrasound biomicroscopy (UBM) and that histopathological analysis would usually confirm the correct type identified by the imaging technique [2]. An example of the former comes from studies showing that sclerocornea (total corneal opacification) were correctly diagnosed by UBM to be Peters' anomaly, the most common CCO sub-type seen in the clinic [2,8–10].

Development of the cornea and molecular players underpinning CCO are poorly understood. Gene expression profiling is a technique that has been effective in identifying targets in the development of ocular tissues and congenital diseases in the lens [11], cornea [12], and retina [13]. RNA-Seq is the most recent platform and is considered better than the usually employed microarrays, as it accurately quantifies RNA transcripts directly [14,15]. However, it has rarely been performed for pediatric tissues of ocular origin. We report a case using UBM, anterior-OCT (Optical coherence tomography) and histological analysis to confirm CCO from a pediatric case of Fanconi anemia (FA). This is a rare (1–5 cases/million), autosomal recessive disorder arising from excess chromosomal breakage, where the characteristics are progressive pancytopenia, elevated risk for tumors (leukemia and solid), and congenital abnormalities - short stature, limb malformations (radial aplasia, thumb aplasia/hypoplasia, or duplicated thumb), skin pigmentation and abnormalities in cardiac, renal, gastrointestinal, endocrine and neuronal development [16]. Ocular manifestations in 48% of cases primarily include short-almond-shaped palpebral fissures, hyper- or hypotelorism, ptosis, microphthalmia and epicanthal folds, with isolated cases of congenital glaucoma, cataract, uveal or optic disc vasculopathy, retinoblastoma [17] and corneal clouding [18]. Comparative RNA-Seq analysis of the opaque cornea from our patient with FA to demonstrate gene expression differences in the affected tissue, including metabolic enzymes of glycosaminoglycans, leads us to a novel mechanism in causation of CCO and uncovering of two related players underpinning CCO.

* Corresponding author at: UPMC Children's Hospital of Pittsburgh, 400 45th St Faculty Pavilion, Suite 5111, Pittsburgh, PA 15201, USA.
E-mail address: bkc10@pitt.edu (B.K. Chauhan).

https://doi.org/10.1016/j.ymgmr.2021.100712
Received 27 November 2020; Received in revised form 15 January 2021; Accepted 16 January 2021

2. Case report

A female pediatric patient diagnosed with FA and poor vision was referred to a pediatric ophthalmologist (K.K.N.) for evaluation at the Eye Center of Children's Hospital of Pittsburgh. The patient, at 23 months-old, presented with blurred vision, microphthalmia, peripheral scleralization, microcorneas (Fig. 1A), a visible ectropion uvea, and pendular nystagmus. Upon examination under anesthesia (EUA), she had clear evidence of anterior segment developmental anomalies (ASDA), where the right cornea was more opaque (Fig. 1B) and displayed a distinct central leukoma. The patient had normal flash visual evoked potentials (VEP). Anterior OCT findings in the right eye showed dehiscence of the Descemet membrane (Fig. 1C) and in the left eye an area of irregularity in the central cornea (Fig. 1D), and hyper-reflective regions observed in both stroma confirmed regions of haze (Fig. 1C-D). UBM revealed iridiocorneal adhesions in both eyes (Fig. 1E-G). Axial lengths were 15 mm

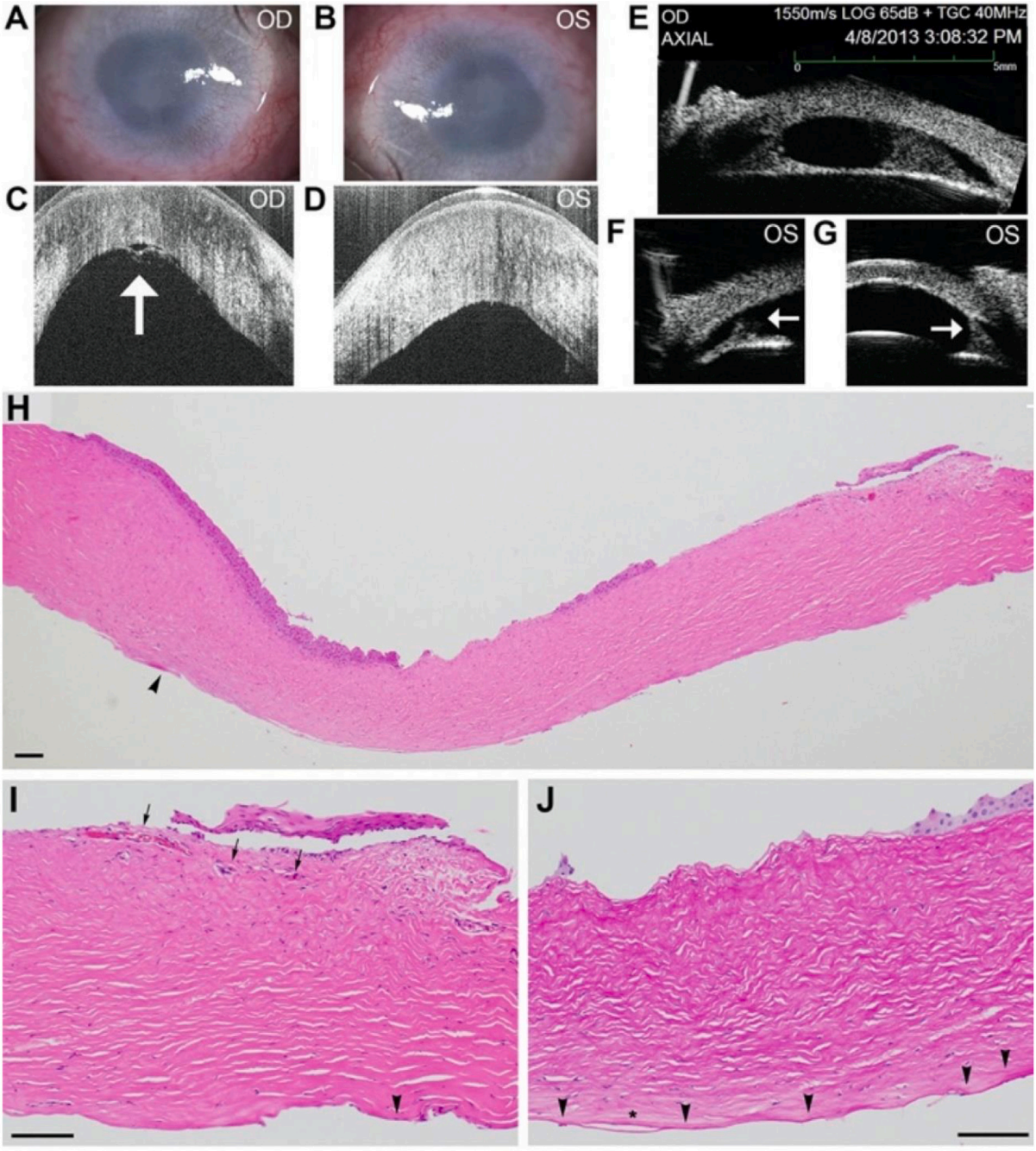

Fig. 1. A-B, microcornea, peripheral scleralization, and corneal opacity in each of the right and left eyes; C—D, dehiscence of the Descemet membrane in the right eye (arrow) and central posterior segment irregularity in the left eye cornea by OCT, with hyper-reflective regions in both stroma demonstrating corneal haze; and *E*-G, iridiocorneal adhesions displayed in both eyes (arrows in F-G for left eye) by ultrasound biomicroscopy (UBM). H, Paraffin-embedded hematoxylin and eosin-stained section of the patient's cornea reveals disruption of the lamellar architecture and absence of Bowman's layer. There is central stromal thinning, and only peripheral segments of normal thickness Descemet's membrane are noted (arrowhead). I, Higher magnification image of the peripheral cornea reveals abnormal stromal architecture accompanied by blood vessels (arrows) as noted in the clinical photographs. Endothelial cells are only focally noted (arrowhead) and Descemet's membrane is attenuated and often difficult to discern. J, Periodic acid–Schiff staining reveals the presence of unusually thin Descemet's membrane (arrowheads) that is sometimes split (asterisk) or detached from the stroma (color).

OS and 14.5 mm OD. Her raised intracranial pressure was treated with ventriculoperitoneal (VP) shunts. She had a lid lift on her left lid and, thereafter, a left fixation preference. Penetrating keratoplasty (PKP), with 6 mm donor trephine on a 5 mm host cornea, and four peripheral iridotomies were performed on the right eye. The patient started on antibiotic/steroid combination drops eight times daily, with eye ointment at night and cyclopentolate (1%) three times daily. Three months later, her right eye was treated for esotropia by right medial rectus recession (4 mm) and lateral rectus resection (5 mm). She began to prefer right eye for fixation. The last VEP showed same signal amplitude, but slight increase in latency maybe due to her aversion to spectacles. Systemic anomalies included short stature, absent radius, microcephaly, dysplastic kidneys, which are established signs for Fanconi anemia [19], in addition to bilateral congenital hip dislocation (CHD), a closed atrial-septal defect (ASD) leaving a patent foramen ovale (PFO), and corpus collosum partial agenesis. The ocular family history noted cataracts and nystagmus, and non-ocular noted cancer and rheumatoid arthritis.

The pathology report on the right eye opaque cornea revealed five notable observations: extensive regions lacking Bowman's membrane (Fig. 1H), central corneal thinning, disorganization and vascularization of the corneal stroma (Fig. 1I), irregular and attenuated Descemet's membrane with paucity of corneal endothelial cells (Fig. 1I-J), and keratinization of the corneal epithelium. The first three findings confirmed the relevant OCT observations (Fig. 1C-D).

The patient was diagnosed with Fanconi anemia based on positive DEB (patient: 3.66; normal: 0–0.3) and MMC (patient: 4.26; normal: 0.06–0.24) chromosome breakage tests. The FA gene sequencing panel showed a heterozygous mutation in *FANCD2* (c.1278 + 3_1278 + 6delAAGT), in addition to single allele mutations of unknown clinical significance in *FANCC* (c.77C > T (p.S26F) and *FANCM* (c.4516-5_4516-2delCTTA.

3. Materials and methods

3.1. Clinical procedures

Case note of patient presenting at UPMC Children's Hospital of Pittsburgh were retrospectively reviewed, including best corrected visual acuity (BCVA), refraction, intraocular pressure (IOP), fundus appearance, and anterior segment phenotype. Slit-lamp biomicroscopy, electrophysiological and optical coherence tomography (OCT) findings were also recorded.

3.2. Tissue samples

Control tissues for the study were taken from an age-matched eyeball (The San Diego Eye bank®). The donor eyeball, at 3 yrs. 10-month-old, was from a male with history of autosomal dominant polycystic kidney disease (ADPKD) associated with Caroli syndrome. Affected patient (ACo), from which informed consent was obtained, and normal donor (Co) corneal tissues were extracted and collected in accordance with the protocol approved by the University of Pittsburgh Institutional Review Board (PRO13090514).

3.3. RNA extraction

Cornea from donor eyeball and affected corneal tissue from the patient (extracted during surgery) were immediately submerged in 1.5 ml RNA*later* (Thermo Fisher Scientific Inc.) aliquots in 2 ml tubes, placed on ice, and stored at −20 °C. Each tissue was cut to small pieces (~ 2 mm), washed with PBS and 600 μl buffer RLT with β-mercaptoethanol at 1/10th volume added (Qiagen RNAeasy Mini kit). They were efficiently disrupted using MagNA Lyser Green Beads (prewashed in concentrated nitric acid) and the MagNA lyser instrument (Roche) using 3 cycles of 20 s disruption and 20 s on ice. Resulting lysates were centrifuged for 2 mins at full speed, supernatants pipetted into fresh 1.5 ml microfuge tubes, and homogenized using the QIAshredder columns (2 mins spin at 13,000 rpm). Supernatants were loaded onto RNeasy mini spin columns, centrifuged (15 s at 8000 rpm), columns washed, buffered and then RNase-free water added prior to 1 min centrifugation at 8000 rpm to elute tissue RNA. The last step was repeated using 30 μl of RNase-free water. Yield and purity of eluents were assessed using the Nano-drop 2000C (Thermo Fisher Scientific Inc).

3.4. RNA library preparation, HiSeq sequencing and data-mining

RNA library preparations, sequencing reactions, and data conversion were conducted at GENEWIZ, LLC. (South Plainfield, NJ, USA; see Supplementary data).

Quality control of RNA-Seq reads were assessed using three criteria: percentage of sample total reads with Phred scores between 30 and 40 (measure base-calling reliability, where score of 30–40 indicates 99.9–99.99% accuracy of a base call [20]), GC content bias, and 70–90% of reads mapping to the human reference genome (hg38) [21]. The CLC Genomics workbench 9.5 program (CLC Bio, Aarhus, Denmark, http://www.clcbio.com/) was used to map genes to hg38 (https://genome.ucsc.edu/ cgi.bin/hgGateway?db = hg38). Gene expression value for each gene, the TPM (Transcripts Per Kilobase Million), was normalized for total exon-length and total number of matches in an experiment (i.e. uniquely mapped reads to genes are counted and non-unique matches are distributed per ratio to genes) [22]. T-tests were performed in $\log_2$transformed data to identify genes with significant differences in expression between phenotypes (p value < 0.05, and $\geq \pm 1.5$-fold differences between phenotypes), and filtered genes were examined by functional analysis using the Ingenuity Pathway Analysis (IPA; Ingenuity Systems, Mountain View, CA; www.ingenuity.com). Comparative transcriptome analysis was performed by comparing our misregulated gene lists to compendium of gene expression studies curated in the correlation engine BaseSpace (Illumina, Inc., San Diego, CA). Common gene expression variation lists between studies were generated by placing misregulated gene lists into a Venn diagram using the web program: Bioinformatics & Evolutionary Genomics (http://bioinformatics.psb.ugent.be/ webtools/Venn/).

4. Results

4.1. Corneal transcriptome of FA patient confirms opaque profile at molecular level and fibrosis

To determine the molecular underpinnings of CCO in FA, we chose comparative RNA-Seq analysis of our affected patient cornea (ACo) versus an age-matched normal donor cornea (Co).

Examination of the Co transcriptome confirmed it represents cornea at the molecular level, as it contains three corneal-enriched keratins in the top 20 highly-expressed genes (*KRT12*, *KRT5*, and *KRT3* [23,24]) and other corneal-specific genes (including the corneal-specific crystallin *ALDH3A1* [25], *CLU* that is highly-expressed in the corneal epithelium [26] and the highly-specific corneal stromal stem cell marker *NT5E (CD73)* [27]; Table S1). Twelve genes in the top 20 highly-expressed genes are members of the ATP-generating mitochondrial genes, which we suggest are primarily expressed by the corneal endothelium to maintain corneal dehydration and, thus, transparency through ionic pumps [28]. The above findings in the Co transcriptome strongly suggest it represents corneal tissue.

Comparative RNA-Seq analysis was conducted to confirm cloudy corneas, at the molecular level in the ACo transcriptome. We focused on corneal stroma-specific genes, as this layer exhibited regions of haze in our patient (Fig. 1C-D, H, I). Out of the 20 highly expressed genes in the normal cornea (Table S1), 3 keratins (*KRT12*, *KRT5*, *KRT3*) were downregulated (Table 1). Both *KRT12* and *KRT5* lead to fibrosis when downregulated [29,30], as do *KRT6A* and *KRT17* when upregulated [31]. Collagens, the next large group of stromal extracellular matrix

Table 1
Corneal genes of the stroma misregulated in the ACo transcriptome of the patient. Abbr: ACo, affected cornea; FC, fold-change; n, number; SLRP, small leucine-rich proteoglycan.

Gene	Category	Function in the cornea		ACo FC
KRT12	Keratins	Mutations cause Meesmann epithelial corneal dystrophy	Leads to fibrosis when misregulated	-5.87
KRT5		forms cytoskeleton with KRT12		-2.68
KRT6A		poorly studied		2.98
KRT17		putative corneal stem cell marker		8.02
KRT78				
KRT80				
KRT3				
KRT14				
		Poorly studied		-8635.43
		Poorly studied		-2589.38
		Mutations cause Meesmann epithelial corneal dystrophy		-3.52
		Leads to regeneration of tissue when upregulated		2.06
COL4A4	Collagens	Mutations in *COL4A5* (X-linked), or *COL4A3*		-13.80
COL12A1		and *COL4A4* (autosomal recessive) result in		-6.32
COL4A3		basement membrane disruption and are		-5.29
COL4A5		associated with corneal opacities.		-2.97
COL6A2				-6.03
COL6A1				-2.89
COL3A1				5.33
COL5A1		Mutations lead to collagen VI-like syndromes, which generally leads to extreme corneal thinning and fragility.		2.35
COL1A1		Upregulation of these genes results in immune responses leading to fibrosis in many organs and tissues, such as kidney, liver, lungs and skin. Col5 is a minor collagen that usually intercalates with Col1, a major collagen.		2.28
LAMA5	Laminin	Mutation causes complex ECM syndrome.		-14.61
LUM	SLRP	Class II SLRP member, made of keratan sulfate proteoglycans, and recognized as major component of the corneal stroma. It contributes to correct formation of collagen fibrils and promotes cell adhesion and migration. In tissue fibrosis (e.g. lung, colon), lumican upregulation promotes fibrocyte differentiation.		3.67

(ECM) proteins, were observed to be mainly downregulated, but one group was upregulated (*COL3A1*, *COL5A1*, *COL1A1*). This group of collagens are known to lead to fibrosis when overexpressed [32–34]. *LUM* (SLRP family member) was found to be significantly upregulated, which consequently also results in a fibrotic response [35].

We next analyzed expression variation in enzymes associated with either glycosaminoglycan (GAG) metabolism or glycosylation (Table 2), particularly downregulated expression as their effects are known. We found all GAG chains (chondroitin sulfate (CS), dermatan sulfate (DS), keratan sulfate (KS), heparan sulfate (HS)) are affected, which reportedly leads to corneal clouding/opacities (*GUSB*, *IDUA*, *GALNS*) [36–38]. For anabolic enzymes, *CHST1* and *CHST6* (KS chains) were significantly downregulated which both contribute to corneal thinning when their expression is reduced [39,40]. Analysis of upregulated GAG metabolic enzymes associated with HA, only *HYAL1* (3.35) and *HAS2* (75.27) were significantly upregulated. The former generates pro-inflammatory hyaluronan fragments [41], whilst the latter partakes in fibrosis of various tissues when upregulated [42]. We found *COLGALT2* as the only glycosylation enzyme concerned with collagen glycosylation that was significantly affected. With glycoprotein glycosylation in the corneal stroma [43], we found twice as many o-glycosylation enzymes at serine/threonine bases (*B3GALT4*, *GALNT7*, *ST6GALNAC6*, *B3GAL NT2*, *B4GALNT3*, *GALNT18*) are downregulated than those involved in n-glycosylation at asparagine bases (*B4GALT5*, *A4GALT*, *B4GALT4*). Both lead to diminished lubrication of the corneal surface and subsequent epithelial keratinization.

To summarize, results from expression variation in the ACo transcriptome confirm an opaque cornea due to downregulation of corneal-specific genes that lead to opacities (*KRT12*, *KRT3*, *COL4A4*, *COL4A5*, *COL4A3*, *GUSB*, *IDUA*, *GALNS*), corneal thinning (*COL12A1*, *COL6A2*, *COL6A1*, *CHST1, CHST6*) and keratinization of the corneal epithelium (*B3GALT4*, *GALNT7*, *ST6GALNAC6*, *B3GALNT2*, *B4GALNT3*, *GALNT18*, *B4GALT5*, *A4GALT*, *B4GALT4*). In addition, the ACo transcriptome shows an abundance of fibrotic/inflammatory responses (downregulation of *KRT12*, *KRT5*, *KRT6A*, *KRT17, CHI3L1, CLU* and upregulation of *COL3A1*, *COL5A1*, *COL1A1*, *LUM, HAS2*).

4.2. Comparison of patient corneal transcriptome variation to those from anemia-related studies uncovers two important genes in fibrosis and wound-healing

To identify the cause of the corneal fibrosis event in our patient corneas, we employed comparative transcriptome variation analysis (COTVA). This technique has been greatly facilitated by the creation of the Illumina BaseSpace® correlation engine, which permits large-scale pairwise comparisons of variation in a study transcriptome to those from 22,562 other gene expression studies [44]. Using this correlation engine, ACo transcriptome variation compared favorably with those from two anemia-related studies (Fig. S1). The first study (GSE17233), analyzing peripheral blood transcriptome variation between one normal individual and two FA patients with undescribed ocular anomalies [45], had 67 common upregulated genes (p-value = 0.0035) and 240 downregulated genes in common (p-value = 1.1e-19) (Fig. S1A). The other study (GSE56088), analyzing erythroid progenitor cell transcriptomes cultured for 7 days between beta-thalassaemia patients and healthy controls, had 776 common upregulated genes (p-value = 1.7e-15) and 968 downregulated genes (p-value = 5.3e-18) (Fig. S1B). Common misregulated genes amongst these 3 studies were identified by placing each study misregulated genes into a Venn diagram format (Fig. S1C). Analysis of the resulting eighteen common genes (Table S2) uncovered the top common downregulated gene as *ZBTB7B*, which is a zinc finger transcription factor that prevents fibrosis by repressing type I collagen genes- established marker of fibrosis [46–48]. *GRN*, a growth factor and potent regulator of wound-healing [49], is another key common downregulated gene.

4.3. Confirmation of ZBTB7B as anti-fibrotic and GRN as wound-healing agents in the cornea

We looked at expression of both genes amongst four ocular tissues, specifically the cornea, lens, optic nerve and retina, and both were found to be significantly highly expressed in the cornea relative to the other tissues (Fig. 2A). To analyze their expression during cornea development, we searched publicly available gene expression studies in the NCBI Gene Expression Omnibus (GEO, http://www.ncbi.nlm.nih.gov/geo/). Two microarray analyses (GSE121044 and GSE43155) were identified that follow gene expression across embryonic and postnatal stages of mouse corneal development [50,51]. We found both genes increased expression during the prenatal stages (from GSE121044; Fig. 2B), where both peaked at ~E15.5 (from GSE43155; Fig. 2C) but *ZBTB7B* also increased steadily during the postnatal period.

A search in NCBI GEO for gene expression studies of the corneal epithelia in connection to fibrosis and wound-healing revealed 2 relevant studies. Dataset GSE43381 identifies genes enriched in mouse cornea, bladder, esophagus, lung, proximal small intestine, skin,

Table 2
Glycosaminoglycan (GAG) catabolic and anabolic enzymes, in addition to glycosylation enzymes, misregulated in the ACo transcriptome. Abbr: ACo, affected cornea; CS, chondroitin sulfate; DS, dermatan sulfate; E, embryonic day; FC, fold-change; n, number; HS, heparan sulfate; KS, keratan sulfate; MPS, mucopolysaccharidosis; PG, proteoglycan.

	Gene	Enzyme group	Target PG (backbone)	Corneal mutant phenotype (A)/null phenotype (B)/corneal function (C)	ACo FC (n)
A.	*GALNS*	catabolic	KS, CS	corneal clouding in MPS IVa (Morquio syndrome B)	-1961.16
	NAGLU		HS	clear corneas in MPS III (Sanfilippo B syndrome) if basement membranes normal	-992.84
	IDUA		DS, HS	corneal clouding in MPS I (Hurler-Scheie syndrome)	-5.63
	GUSB		CS, DS, HS	corneal opacity in MPS VII (Sly syndrome)	-4.15
	HYAL1		HA	unknown	3.35
B.	*CHST7*	anabolic	CS	unknown	-704.71
	CSGALNACT2		CS, DS	normal and fertile	-11.34
	CHPF2		CS		-6.34
	CHST15		CS DS		-3.13
	HAS2		HA	E9.5-10	75.27
	HS6ST2		HS	normal till 20 months and fertile	-567.73
	NDST2		HS	normal and fertile	-7.93
	HS6ST1		HS	E15.5	-2.66
	B3GAT3		HS, CS	8-cell stage	-2.61
	NDST1		HS	before or at birth	-2.55
	HS2ST1		HS	neonatal period	-2.35
	CHST1		KS	corneal thinning when downregulated	-1106.21
	CHST6		KS	corneal thinning in Macular Corneal Dystrophy (MCD)	-2.13
C.	*COLGALT2*	glycosylation		glycosylation of collagen	-3.61
	B3GALT4			O-glycosylation of proteins	-2277.63
	GALNT7				-28.73
	ST6GALNAC6				-10.96
	B3GALNT2				-6.95
	B4GALNT3				-5.13
	GALNT18				-3.43
	B4GALT5			N-glycosylation of proteins	-2.48
	A4GALT				-2.22
	B4GALT4				-2.14

stomach, and trachea epithelia [51]. We found, unexpectedly, high expression of *ZBTB7B* and *GRN* in the cornea, lung and trachea epithelia relative to those found in the bladder, esophagus, and stomach epithelia (Fig. S2A—B). Expression of several important anti-inflammatory players that prevent fibrosis, *IL4*, *IL10*, *IL13* and *TNFα*, were also found to follow the same pattern (Fig. S2A). These results suggest *ZBTB7B* and *GRN* are highly expressed in those tissues where anti-inflammatory responses are significant.

This above finding led to two hypotheses, where the first was that downregulation of the anti-fibrotic factor *ZBTB7B* in injured corneas leads to fibrosis in the tissue that subsequently leads to opacities. Confirmation of this theory comes from the microarray-based study on chemical burns (silver nitrate application) to mice cornea that results in representative gene expression changes in the lacrimal gland [52]. Both corneas became opaque, and corresponding gene expression changes in the lacrimal gland reflective of expression variation in the cornea were examined post-injury compared to non-injured mice. We uncovered significant downregulation in *ZBTB7B* (−2.65) in the lacrimal gland 8 hrs post-injury (Fig. S2C), thus confirming our hypothesis that *ZBTB7B* downregulation in corneal injury may contribute to opacities in the tissue. A study comparing scleroderma (fibrotic skin) fibroblasts to normal ones where the fibrotic marker *COL1A1* was shown to be upregulated upon *ZBTB7B* and *Sp1* downregulation [53] further confirms our hypothesis, because the ACo transcriptome also shows downregulation of *ZBTB7B*, *Sp1* and upregulation of *COL1A1* (Fig. S2D).

In the second hypothesis, we propose *GRN* is important for wound-healing in damaged corneas. A study showing this comes from analysis of corneal wound-healing after ethyl pyruvate addition to culture

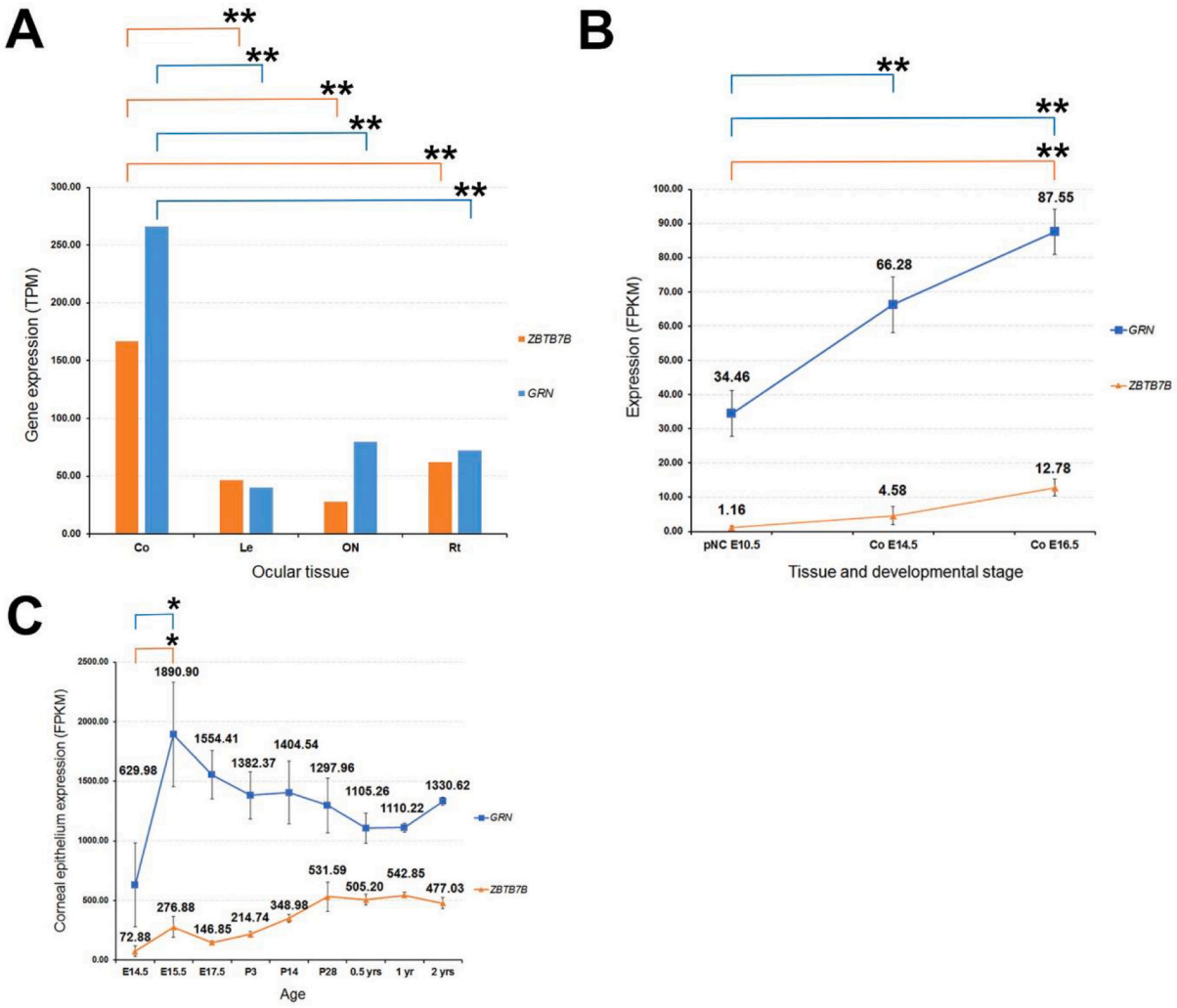

Fig. 2. A, Expression data for *ZBTB7B* and *GRN* in ocular tissues of pediatric donor eye through RNA-Seq; B, *ZBTB7B* and *GRN* expression during early corneal development in the mouse from E10.5 – E16.5 (GEO dataset: GSE121044); C, *ZBTB7B* and *GRN* expression in the mouse corneal epithelia from E14.5–2 yrs. (GEO dataset: GSE43155). Abbreviations: Co, cornea; CoE, corneal epithelium; E, embryonic day; P, postnatal day; pNC, periocular neural crest; SK, stromal keratocytes. * represents $p < 0.05$; ** represents $p < 0.005$.

medium where prior *TGFβ1* treatment leads to corneal keratocytes forming myofibroblasts [54]. Subsequent ethyl pyruvate addition leads to modifying the *TGFβ1*-driven transition of keratocytes to myofibroblasts by inhibiting upregulation of profibrotic genes, thus replicating the wound-healing response. We identify a significant increase in *GRN* expression in the dataset after ethyl pyruvate addition (Fig. S2E), thus confirming *GRN* in the cornea contributes to wound-healing.

5. Discussion

This is the first report of RNA-Seq gene expression analysis on an opaque cornea from a patient with FA. Clinical examination revealed bilateral microcornea in the patient (Fig. 1A), which has been reported in 55–100% of FA seen in the clinic [17,55] whereas CCO has not been previously described in FA. External exam and anterior-OCT established corneal haze in both eyes with increased opacity in the right cornea (Fig. 1B, C-D). Histopathology analysis confirmed the anterior-OCT findings (Fig. 1C-D) that the haze was in the corneal stroma (Fig. 1I), in addition to uncovering corneal membranes were disrupted (Fig. I-J), central cornea was irregular, and the epithelium was keratinized.

Findings of opacity in the corneal stroma directed our subsequent RNA-Seq analysis towards proteins highly expressed there (Table 1), which was determined from those that were found to be highly expressed in a normal cornea (Table S1). Certain keratins (*KRT12*, *KRT5*, *KRT3*) were downregulated and some upregulated (*KRT6A* and *KRT17*), as were specific collagens (*COL3A1*, *COL5A1*, *COL1A1*), which previous studies demonstrated lead to fibrosis [29–34]. The SLRP family member *LUM*, proven to result in fibrosis when upregulated [35,56], was also over-expressed. These findings suggested the patient cornea has undergone opacity-generating fibrosis, which has been proven in the cornea when infected, injured or post-surgery [57,58].

Features of the patient corneal histopathology were confirmed in the transcriptome when we analyzed expression variation in GAG metabolism or glycosylation enzymes (Table 2). This approach was taken as major fibrous proteins and proteoglycans in the corneal stroma [59] are either heavily dependent on glycosylation or contain GAGs respectively. We found catabolic enzymes targeted all GAG chains and produce corneal haze when downregulated (*GUSB*, *IDUA*, *GALNS*) [36–38]. *NAGLU* is the only exception, which has exhibited opaque corneas in MPS III only upon massive HS accumula- tion where basement membrane disruption was also evident [60]. Interesting anabolic enzymes were those targeting KS chains (*CHST1* and *CHST6*), which cause corneal thinning when downregulated [39,40]. Nine members of o- and n-glycosylation enzymes were downregulated (*B3GALT4*, *GALNT7*, *ST6GALNAC6*, *B3GALNT2*, *B4GALNT3*, *GALNT18*), which results in epithelial keratinization from decreased corneal surface lubrication

[43]. Upregulated GAG metabolic enzymes were associated with hyaluronan metabolism, *HYAL1* and *HAS2*; the first generates pro-inflammatory hyaluronan fragments [41] and the second partakes in tissue fibrosis when upregulated [42], thus adding further evidence on opacity-causing fibrosis in the patient cornea.

To determine molecular players of fibrosis in the patient cornea, we conducted comparative transcriptome analysis using the Illumina BaseSpace® correlation engine. Two anemia-related studies had a significant correlation with the affected cornea transcriptome (Fig. S1A—B)), which were considered reasonable as blood and parts of the cornea (i.e. stroma) are derived from embryonic mesoderm [61]. For the same reason, fibrotic genes could be identified from these comparisons without corneal opacities being prevalent in FA or anemia-related disease. When common misregulated genes between these datasets were placed in a Venn diagram (Fig. S1C), *ZBTB7B* and *GRN* were identified (Table S2) that play roles as anti-fibrotic and wound repair factors, respectively [47,62].

We showed that *ZBTB7B* and *GRN* are highly expressed, together with anti-inflammatory markers (*IL4*, *IL10*, *IL13* and *TNFα)*, in tissue epithelia where fibrosis would be considered fatal (lungs and trachea [63,64]) in contrast to epithelia where fibrosis is not fatal (bladder and stomach) (Fig. S2A—B). We also show that they are both highly expressed in the cornea (Fig. 2A), therefore indicating their importance in preventing fibrosis and, therefore, blindness by opacity formation. In demonstrating *ZBTB7B* has a role in preventing fibrosis and corneal opacities, we focused on a study in which rabbit eyes were exposed to chemical burns through silver nitrate application and reflective gene expression changes in the cornea were monitored by gene expression analysis of the lacrimal glands [52]. Gene expression changes in the lacrimal glands reflective of those in the cornea has long been proven [65–70]. Our processing of the raw data from lacrimal gene expression changes to show reduction of *ZBTB7B* in this model of chemical burns-inducing corneal opacities (Fig. S2C—D) is thus evident that decrease in the factor may play a role in CCO causation. For *GRN* role in wound-healing, we choose a *TGFβ1*-induced fibrosis study where conversion of keratocytes to myofibroblasts was reversed by ethyl pyruvate addition [54]. We uncovered that *GRN* is increased (Fig. S2E) in the wound-healing type reversal, therefore suggesting it could be involved in wound-healing of the cornea.

Expanding the number of CCO cases to demonstrate basement membrane disruption and analyze gene expression through RNA-Seq technologies to establish opacity-causing fibrosis would be a necessary step forward in confirming our hypothesis for CCO causation. Studies of mice where *ZBTB7B/GRN* would be specifically reduced in the developing cornea to induce opacity-causing fibrosis and rescuing the ensuing corneal opacity through over-expression of *GRN/ZBTB7B* would prove the roles of these factors in corneal opacity.

Supplementary data to this article can be found online at https://doi.org/10.1016/j.ymgmr.2021.100712.

Data sharing statement

Co and ACo RNA-seq datasets have been deposited in NCBI's Gene Expression Omnibus [71] and are accessible at GSE (GSE162236).

Declaration of Competing Interest

The authors declare no conflict of interest.

Acknowledgments

This work is supported by The Jack Buncher Foundation to K.N.N. and B.K.C., National Institutes of Health CORE Grant P30 EY008098, Eye and Ear Foundation of Pittsburgh, Pennsylvania, USA, and unrestricted grant from Research to Prevent Blindness, New York, New York, USA. Software licensed through the Molecular Biology Information Service, Health Sciences Library System of the University of Pittsburgh, was used for data analysis and assisted by Dr. Ansuman Chattopadhyay. We thank Martha L. Funderburgh and James L. Funderburgh for assistance and technical expertise on RNA extraction from the cornea.

References

[1] J.M. Kurilec, G.W. Zaidman, Incidence of Peters anomaly and congenital corneal opacities interfering with vision in the United States, Cornea 33 (2014) 848–850.
[2] K.K. Nischal, J. Naor, V. Jay, L.D. MacKeen, D.S. Rootman, Clinicopathological correlation of congenital corneal opacification using ultrasound biomicroscopy, Br. J. Ophthalmol. 86 (2002) 62–69.
[3] K.K. Nischal, Genetics of Congenital Corneal Opacification–Impact on Diagnosis and Treatment, Cornea 34 (Suppl. 10) (2015) S24–S34.
[4] D. Trief, M.C. Marquezan, C.J. Rapuano, C.R. Prescott, Pediatric corneal transplants, Curr. Opin. Ophthalmol. 28 (2017) 477–484.
[5] K.K. Nischal, Congenital corneal opacities - a surgical approach to nomenclature and classification, Eye 21 (2007) 1326–1337.
[6] K.K. Nischal, A new approach to the classification of neonatal corneal opacities, Curr. Opin. Ophthalmol. 23 (2012) 344–354.
[7] J.S. Weiss, H.U. Moller, A.J. Aldave, B. Seitz, C. Bredrup, T. Kivela, F.L. Munier, C. J. Rapuano, K.K. Nischal, E.K. Kim, J. Sutphin, M. Busin, A. Labbe, K.R. Kenyon, S. Kinoshita, W. Lisch, IC3D classification of corneal dystrophies–edition 2, Cornea 34 (2015) 117–159.
[8] C. Shigeyasu, M. Yamada, Y. Mizuno, T. Yokoi, S. Nishina, N. Azuma, Clinical features of anterior segment dysgenesis associated with congenital corneal opacities, Cornea 31 (2012) 293–298.
[9] R.A. Rezende, U.B. Uchoa, R. Uchoa, C.J. Rapuano, P.R. Laibson, E.J. Cohen, Congenital corneal opacities in a cornea referral practice, Cornea 23 (2004) 565–570.
[10] V.C. Parmley, K.G. Stonecipher, J.J. Rowsey, Peters' anomaly: a review of 26 penetrating keratoplasties in infants, Ophthalmic Surg. 24 (1993) 31–35.
[11] B.K. Chauhan, N.A. Reed, W. Zhang, M.K. Duncan, M.W. Kilimann, A. Cvekl, Identification of genes downstream of Pax6 in the mouse lens using cDNA microarrays, J. Biol. Chem. 277 (2002) 11539–11548.
[12] J. You, S.M. Corley, L. Wen, C. Hodge, R. Hollhumer, M.C. Madigan, M.R. Wilkins, G. Sutton, RNA-Seq analysis and comparison of corneal epithelium in keratoconus and myopia patients, Sci. Rep. 8 (2018) 389.
[13] S. Kaur, S. Gupta, M. Chaudhary, M.A. Khursheed, S. Mitra, A.J. Kurup, R. Ramachandran, let-7 MicroRNA-Mediated Regulation of Shh Signaling and the Gene Regulatory Network Is Essential for Retina Regeneration, Cell Rep. 23 (2018) 1409–1423.
[14] J. Xu, S. Thakkar, B. Gong, W. Tong, The FDA's Experience with Emerging Genomics Technologies-Past, Present, and Future, AAPS J. 18 (2016) 814–818.
[15] S. Zhao, W.P. Fung-Leung, A. Bittner, K. Ngo, X. Liu, Comparison of RNA-Seq and microarray in transcriptome profiling of activated T cells, PLoS One 9 (2014) e78644.
[16] H. Kook, Fanconi anemia: current management, Hematology 10 (Suppl. 1) (2005) 108–110.
[17] A.L. Tornquist, L. Martin, J. Winiarski, K.T. Fahnehjelm, Ocular manifestations and visual functions in patients with Fanconi anaemia, Acta Ophthalmol. 92 (2014) 171–178.
[18] J.J. Lee, L.M. Tripi, R.W. Erbe, S. Garimella-Krovi, J.E. Springate, A mitochondrial DNA deletion presenting with corneal clouding and severe Fanconi syndrome, Pediatr. Nephrol. 27 (2012) 869–872.
[19] J. Bhandari, P.K. Thada, Y. Puckett, Fanconi Anemia, StatPearls, Treasure Island (FL), 2020.
[20] B. Ewing, P. Green, Base-calling of automated sequencer traces using phred. II. Error probabilities, Genome Res. 8 (1998) 186–194.
[21] A. Conesa, P. Madrigal, S. Tarazona, D. Gomez-Cabrero, A. Cervera, A. McPherson, M.W. Szczesniak, D.J. Gaffney, L.L. Elo, X. Zhang, A. Mortazavi, A survey of best practices for RNA-seq data analysis, Genome Biol. 17 (2016) 13.
[22] A. Mortazavi, B.A. Williams, K. McCue, L. Schaeffer, B. Wold, Mapping and quantifying mammalian transcriptomes by RNA-Seq, Nat. Methods 5 (2008) 621–628.
[23] H. Alam, L. Sehgal, S.T. Kundu, S.N. Dalal, M.M. Vaidya, Novel function of keratins 5 and 14 in proliferation and differentiation of stratified epithelial cells, Mol. Biol. Cell 22 (2011) 4068–4078.
[24] Y. Sasamoto, R. Hayashi, S.J. Park, M. Saito-Adachi, Y. Suzuki, S. Kawasaki, A. J. Quantock, K. Nakai, M. Tsujikawa, K. Nishida, PAX6 Isoforms, along with Reprogramming Factors, Differentially Regulate the Induction of Cornea-specific Genes, Sci. Rep. 6 (2016) 20807.
[25] T. Estey, J. Piatigorsky, N. Lassen, V. Vasiliou, ALDH3A1: a corneal crystallin with diverse functions, Exp. Eye Res. 84 (2007) 3–12.
[26] K. Nishida, S. Kawasaki, W. Adachi, S. Kinoshita, Apolipoprotein J expression in human ocular surface epithelium, Invest. Ophthalmol. Vis. Sci. 37 (1996) 2285–2292.
[27] P.F. Choong, P.L. Mok, S.K. Cheong, K.Y. Then, Mesenchymal stromal cell-like characteristics of corneal keratocytes, Cytotherapy 9 (2007) 252–258.
[28] W.M. Bourne, Biology of the corneal endothelium in health and disease, Eye (Lond) 17 (2003) 912–918.
[29] H. Hassan, C. Thaung, N.D. Ebenezer, G. Larkin, A.J. Hardcastle, S.J. Tuft, Severe Meesmann's epithelial corneal dystrophy phenotype due to a missense mutation in the helix-initiation motif of keratin 12, Eye 27 (2013) 367–373.

[30] W. Zuo, T. Zhang, D.Z. Wu, S.P. Guan, A.A. Liew, Y. Yamamoto, X. Wang, S.J. Lim, M. Vincent, M. Lessard, C.P. Crum, W. Xian, F. McKeon, p63(+)Krt5(+) distal airway stem cells are essential for lung regeneration Nature 517 (2015) 616-620.
[31] J. Song, H. Zhang, Z. Wang, W. Xu, L. Zhong, J. Cao, J. Yang, Y. Tian, D. Yu, J. Ji, J. Cao, S. Zhang, The Role of FABP5 in Radiation-Induced Human Skin Fibrosis, Radiat. Res. 189 (2018) 177–186.
[32] S.A. Jimenez, B. Saitta, Alterations in the regulation of expression of the alpha 1(I) collagen gene (COL1A1) in systemic sclerosis (scleroderma), Springer Semin. Immunopathol. 21 (1999) 397–414.
[33] H. Kuivaniemi, G. Tromp, Type III collagen (COL3A1): Gene and protein structure, tissue distribution, and associated diseases, Gene 707 (2019) 151–171.
[34] G.S. Lei, H.L. Kline, C.H. Lee, D.S. Wilkes, C. Zhang, Regulation of Collagen V Expression and Epithelial-Mesenchymal Transition by miR-185 and miR-186 during Idiopathic Pulmonary Fibrosis, Am. J. Pathol. 186 (2016) 2310–2316.
[35] D. Pilling, V. Vakil, N. Cox, R.H. Gomer, TNF-alpha-stimulated fibroblasts secrete lumican to promote fibrocyte differentiation, in: Proceedings of the National Academy of Sciences of the United States of America 112, 2015, pp. 11929–11934.
[36] B. Kasmann-Kellner, J. Weindler, B. Pfau, K.W. Ruprecht, Ocular changes in mucopolysaccharidosis IV A (Morquio A syndrome) and long-term results of perforating keratoplasty, Ophthalmologica 213 (1999) 200–205.
[37] R.D. Young, P. Liskova, C. Pinali, B.P. Palka, M. Palos, K. Jirsova, E. Hrdlickova, M. Tesarova, M. Elleder, J. Zeman, K.M. Meek, C. Knupp, A.J. Quantock, Large proteoglycan complexes and disturbed collagen architecture in the corneal extracellular matrix of mucopolysaccharidosis type VII (Sly syndrome), Invest. Ophthalmol. Vis. Sci. 52 (2011) 6720–6728.
[38] C. Yuan, E.D. Bothun, D.R. Hardten, J. Tolar, L.K. McLoon, A novel explanation of corneal clouding in a bone marrow transplant-treated patient with Hurler syndrome, Exp. Eye Res. 148 (2016) 83–89.
[39] A.H. Conrad, Y. Zhang, A.R. Walker, L.A. Olberding, A. Hanzlick, A.J. Zimmer, R. Morffi, G.W. Conrad, Thyroxine affects expression of KSPG-related genes, the carbonic anhydrase II gene, and KS sulfation in the embryonic chicken cornea, Invest. Ophthalmol. Vis. Sci. 47 (2006) 120–132.
[40] L. Dudakova, M. Palos, M. Svobodova, J. Bydzovsky, L. Huna, K. Jirsova, A. J. Hardcastle, S.J. Tuft, P. Liskova, Macular corneal dystrophy and associated corneal thinning, Eye (Lond) 28 (2014) 1201–1205.
[41] A. Avenoso, G. Bruschetta, A. D'Ascola, M. Scuruchi, G. Mandraffino, R. Gullace, A. Saitta, S. Campo, G.M. Campo, Hyaluronan fragments produced during tissue injury: A signal amplifying the inflammatory response, Arch. Biochem. Biophys. 663 (2019) 228–238.
[42] Y.M. Yang, M. Noureddin, C. Liu, K. Ohashi, S.Y. Kim, D. Ramnath, E.E. Powell, M. J. Sweet, Y.S. Roh, I.F. Hsin, N. Deng, Z. Liu, J. Liang, E. Mena, D. Shouhed, R. F. Schwabe, D. Jiang, S.C. Lu, P.W. Noble, E. Seki, Hyaluronan synthase 2-mediated hyaluronan production mediates Notch1 activation and liver fibrosis Sci Transl Med 11, 2019.
[43] M.C. Rodriguez Benavente, P. Argueso, Glycosylation pathways at the ocular surface, Biochem. Soc. Trans. 46 (2018) 343–350.
[44] I. Kupershmidt, Q.J. Su, A. Grewal, S. Sundaresh, I. Halperin, J. Flynn, M. Shekar, H. Wang, J. Park, W. Cui, G.D. Wall, R. Wisotzkey, S. Alag, S. Akhtari, M. Ronaghi, Ontology-based meta-analysis of global collections of high-throughput public data, PLoS One 5 (2010).
[45] P. Shyamsunder, K.S. Ganesh, P. Vidyasekar, S. Mohan, R.S. Verma, Identification of novel target genes involved in Indian Fanconi anemia patients using microarray, Gene 531 (2013) 444–450.
[46] H. Tanaka, I. Taniuchi, The CD4/CD8 lineages: central decisions and peripheral modifications for T lymphocytes, Curr. Top. Microbiol. Immunol. 373 (2014) 113–129.
[47] G. Beauchef, N. Bigot, M. Kypriotou, E. Renard, B. Poree, R. Widom, A. Dompmartin-Blanchere, T. Oddos, F.X. Maquart, M. Demoor, K. Boumediene, P. Galera, The p65 subunit of NF-kappaB inhibits COL1A1 gene transcription in human dermal and scleroderma fibroblasts through its recruitment on promoter by protein interaction with transcriptional activators (c-Krox, Sp1, and Sp3), J. Biol. Chem. 287 (2012) 3462–3478.
[48] A.K. Ghosh, Factors involved in the regulation of type I collagen gene expression: implication in fibrosis, Exp Biol Med (Maywood) 227 (2002) 301–314.
[49] P.S. Bansal, M.J. Smout, D. Wilson, C. Cobos Caceres, M. Dastpeyman, J. Sotillo, J. Seifert, P.J. Brindley, A. Loukas, N.L. Daly, Development of a Potent Wound Healing Agent Based on the Liver Fluke Granulin Structural Fold, J. Med. Chem. 60 (2017) 4258–4266.
[50] J. Ma, P. Lwigale, Transformation of the Transcriptomic Profile of Mouse Periocular Mesenchyme During Formation of the Embryonic Cornea, Invest. Ophthalmol. Vis. Sci. 60 (2019) 661–676.
[51] D.N. Stephens, R.H. Klein, M.L. Salmans, W. Gordon, H. Ho, B. Andersen, The Ets transcription factor EHF as a regulator of cornea epithelial cell identity, J. Biol. Chem. 288 (2013) 34304–34324.
[52] Y. Fang, D. Choi, R.P. Searles, W.D. Mathers, A time course microarray study of gene expression in the mouse lacrimal gland after acute corneal trauma, Invest. Ophthalmol. Vis. Sci. 46 (2005) 461–469.
[53] E. Renard, C. Chadjichristos, M. Kypriotou, G. Beauchef, P. Bordat, A. Dompmartin, R.L. Widom, K. Boumediene, J.P. Pujol, P. Galera, Chondroitin sulphate decreases collagen synthesis in normal and scleroderma fibroblasts through a Smad-independent TGF-beta pathway–implication of C-Krox and Sp1, J. Cell. Mol. Med. 12 (2008) 2836–2847.
[54] S.A. Harvey, E. Guerriero, N. Charukamnoetkanok, J. Piluek, J.S. Schuman, N. Sundarraj, Responses of cultured human keratocytes and myofibroblasts to ethyl pyruvate: a microarray analysis of gene expression, Invest. Ophthalmol. Vis. Sci. 51 (2010) 2917–2927.
[55] E.T. Tsilou, N. Giri, S. Weinstein, C. Mueller, S.A. Savage, B.P. Alter, Ocular and orbital manifestations of the inherited bone marrow failure syndromes: Fanconi anemia and dyskeratosis congenita, Ophthalmology 117 (2010) 615–622.
[56] J.R. Hassell, D.E. Birk, The molecular basis of corneal transparency, Exp. Eye Res. 91 (2010) 326–335.
[57] C.S. Medeiros, G.K. Marino, M.R. Santhiago, S.E. Wilson, The Corneal Basement Membranes and Stromal Fibrosis, Invest. Ophthalmol. Vis. Sci. 59 (2018) 4044–4053.
[58] A.A. Torricelli, A. Santhanam, J. Wu, V. Singh, S.E. Wilson, The corneal fibrosis response to epithelial-stromal injury, Exp. Eye Res. 142 (2016) 110–118.
[59] P.N. Lewis, C. Pinali, R.D. Young, K.M. Meek, A.J. Quantock, C. Knupp, Structural interactions between collagen and proteoglycans are elucidated by three-dimensional electron tomography of bovine cornea, Structure 18 (2010) 239–245.
[60] S.C. Lin, F.R. Hu, J.W. Hou, Y.T. Yao, T.R. Wang, P.T. Hung, Corneal opacity and congenital glaucoma associated with massive heparan sulfaturia: report of one case, Acta Paediatr. Taiwan. 40 (1999) 46–49.
[61] P.J. Gage, W. Rhoades, S.K. Prucka, T. Hjalt, Fate maps of neural crest and mesoderm in the mammalian eye, Invest. Ophthalmol. Vis. Sci. 46 (2005) 4200–4208.
[62] Y.P. Zhao, Q.Y. Tian, S. Frenkel, C.J. Liu, The promotion of bone healing by progranulin, a downstream molecule of BMP-2, through interacting with TNF/TNFR signaling, Biomaterials 34 (2013) 6412–6421.
[63] A. Caminati, C. Lonati, R. Cassandro, D. Elia, G. Pelosi, O. Torre, M. Zompatori, E. Uslenghi, S. Harari, Comorbidities in idiopathic pulmonary fibrosis: an underestimated issue, Eur. Respir. Rev. 28 (2019).
[64] A. Almanzar, M. Danckers, Laryngotracheal Stenosis, StatPearls, Treasure Island (FL), 2020.
[65] A. Higuchi, K. Ito, M. Dogru, M. Kitamura, F. Mitani, T. Kawakita, Y. Ogawa, K. Tsubota, Corneal damage and lacrimal gland dysfunction in a smoking rat model, Free Radic. Biol. Med. 51 (2011) 2210–2216.
[66] Y. Ma, S. Zhao, X. Wang, S. Shen, M. Ma, W. Xu, A. Hong, A New Recombinant PACAP-Derived Peptide Efficiently Promotes Corneal Wound Repairing and Lacrimal Secretion, Invest. Ophthalmol. Vis. Sci. 56 (2015) 4336–4349.
[67] J. Schechter, M. Wallace, J. Carey, N. Chang, M. Trousdale, R. Wood, Corneal insult affects the production and distribution of FGF-2 within the lacrimal gland, Exp. Eye Res. 70 (2000) 777–784.
[68] U. Schulze, U. Hampel, S. Sel, L. Contreras-Ruiz, M. Schicht, J. Dieckow, Y. Diebold, F. Paulsen, Trefoil factor family peptide 3 (TFF3) is upregulated under experimental conditions similar to dry eye disease and supports corneal wound healing effects in vitro, Invest. Ophthalmol. Vis. Sci. 55 (2014) 3037–3042.
[69] H.W. Thompson, R.W. Beuerman, J. Cook, L.W. Underwood, D.H. Nguyen, Transcription of message for tumor necrosis factor-alpha by lacrimal gland is regulated by corneal wounding, Adv. Exp. Med. Biol. 350 (1994) 211–217.
[70] S.E. Wilson, Q. Liang, W.J. Kim, Lacrimal gland HGF, KGF, and EGF mRNA levels increase after corneal epithelial wounding, Invest. Ophthalmol. Vis. Sci. 40 (1999) 2185–2190.
[71] R. Edgar, M. Domrachev, A.E. Lash, Gene Expression Omnibus: NCBI gene expression and hybridization array data repository, Nucleic Acids Res. 30 (2002) 207–210.